

Lectin Receptor-like Kinase Signaling during Engineered Ectomycorrhiza Colonization

Him Shrestha ^{1,2} , Tao Yao ² , Zhenzhen Qiao ², Wellington Muchero ², Robert L. Hettich ^{1,2}, Jin-Gui Chen ^{2,*} 
and Paul E. Abraham ^{1,2,*} 

¹ Genome Science and Technology, University of Tennessee-Knoxville, Knoxville, TN 37996, USA

² Biosciences Division, Oak Ridge National Laboratory, Oak Ridge, TN 37831, USA

* Correspondence: chenj@ornl.gov (J.-G.C.); abrahampe@ornl.gov (P.E.A.)

Abstract: Mutualistic association can improve a plant's health and productivity. G-type lectin receptor-like kinase (PtLecRLK1) is a susceptibility factor in *Populus trichocarpa* that permits root colonization by a beneficial fungus, *Laccaria bicolor*. Engineering PtLecRLK1 also permits *L. bicolor* root colonization in non-host plants similar to *Populus trichocarpa*. The intracellular signaling reprogrammed by PtLecRLK1 upon recognition of *L. bicolor* to allow for the development and maintenance of symbiosis is yet to be determined. In this study, phosphoproteomics was utilized to identify phosphorylation-based relevant signaling pathways associated with PtLecRLK1 recognition of *L. bicolor* in transgenic switchgrass roots. Our finding shows that PtLecRLK1 in transgenic plants modifies the chitin-triggered plant defense and MAPK signaling along with a significant adjustment in phytohormone signaling, ROS balance, endocytosis, cytoskeleton movement, and proteasomal degradation in order to facilitate the establishment and maintenance of *L. bicolor* colonization. Moreover, protein–protein interaction data implicate a cGMP-dependent protein kinase as a potential substrate of PtLecRLK1.

Keywords: phosphoproteomics; lectin receptor-like kinase; plant–microbe interaction; symbiosis; ectomycorrhiza colonization



Citation: Shrestha, H.; Yao, T.; Qiao, Z.; Muchero, W.; Hettich, R.L.; Chen, J.-G.; Abraham, P.E. Lectin Receptor-like Kinase Signaling during Engineered Ectomycorrhiza Colonization. *Cells* **2023**, *12*, 1082. <https://doi.org/10.3390/cells12071082>

Academic Editor: Eduardo A. Espeso

Received: 23 February 2023

Revised: 24 March 2023

Accepted: 30 March 2023

Published: 4 April 2023



Copyright: © 2023 by the authors. Licensee MDPI, Basel, Switzerland. This article is an open access article distributed under the terms and conditions of the Creative Commons Attribution (CC BY) license (<https://creativecommons.org/licenses/by/4.0/>).

1. Introduction

Plants coevolve simultaneously with diverse microbial communities [1–4] and establish molecular mechanisms to either permit or prevent the establishment of a particular microorganism [5,6]. Because microbial interactions can benefit plant sustainability and productivity, it is important to understand the genetic and environmental factors that determine interactions and their outcome on plants and their surrounding environments. Understanding the ecological and evolutionary principles governing these interactions provides an opportunity to engineer microbes and plants to achieve more sustainable and productive ecosystems [7] and mitigate risks associated with introducing microbes into non-native environments [8,9].

Quite remarkably, recent studies have shown that a single plant host gene can be genetically engineered to selectively prevent [10] or permit colonization for a particular fungus [11,12]. How these ‘susceptibility factors’ evolved to functionally override all other levels of plant immunity is poorly understood. In a recent study, we applied quantitative trait locus (QTL) mapping in poplar, which is an important biofeedstock for pulpwood, lumber, and bioenergy, and identified a susceptibility factor implicated in fungal root colonization [12]. It was determined that *Populus trichocarpa* encode a G-type lectin receptor-like kinase (PtLecRLK1) that permits root colonization for *Laccaria bicolor*, a beneficial ectomycorrhizal (ECM) fungus that provides poplar soil nutrients and water in exchange for carbon. Most intriguingly, genetically engineering PtLecRLK1 into non-host plants (*Arabidopsis* and switchgrass) fully permits *L. bicolor* plant root invasion and the establishment of intracellular hyphae (referred to as Hartig net), a prerequisite for symbiosis [11,12].

Upon fungal recognition, plasma membrane (PM)-localized receptor-like kinases (RLKs) trigger coordinated signaling pathways for an extensive new transcriptional program in the plant host, particularly in the root, for cellular remodeling and metabolic alterations to accommodate the growing interaction [13–17]. A multi-omics assessment of *PtLecRLK1* transgenic switchgrass roots identified dramatic changes in host transcription and translation, and the concurrent changes in the metabolite abundance that occurred with *L. bicolor* colonization [11]. Engineering *PtLecRLK1* into a switchgrass plant changes its susceptibility to *L. bicolor* by reprogramming the expression of transcripts, proteins, and metabolites associated with intracellular transport, nutrient assimilation, carbohydrate metabolism, cell cycle and wall organization, and defense-related processes. Yet, despite this advancement, it remains to be determined how *PtLecRLK1* recognition of *L. bicolor* alters intracellular signaling to reprogram the host for the development and maintenance of symbiosis. Therefore, the goals of this study were to identify phosphorylation-based signaling associated with *PtLecRLK1* transgenic switchgrass roots and to develop a conceptual model for relevant signaling pathways. To this end, phosphoproteomics data were generated for wild-type and *PtLecRLK1* transgenic switchgrass roots two months post-inoculation with *L. bicolor*.

2. Method

2.1. Plant Fungal Growth and Proteomics Sample Preparation

Switchgrass *PtLecRLK1* transgenic lines were generated as described previously [11]. Transgenic and wild-type switchgrass were co-cultured with *L. bicolor* liquid inoculum. Two-month post-inoculation, root tissues were collected for mass spectroscopy with at least three biological replicates. Each replicate was flash-frozen and ground under liquid nitrogen. Samples were processed for mass spectrometry measurement as described previously [11]. Briefly, the samples were dissolved in lysis buffer containing 4% SDS in 100 mM ammonium bicarbonate (ABC) buffer along with 1X Halt Protease Inhibitor Cocktail (Thermo Scientific; Waltham, MA, USA). The sample mixture was subjected to boiling, sonication, and centrifugation. The supernatant was collected and reduced with 10 mM dithiothreitol for 30 min and subsequently alkylated with 30 mM iodoacetamide in the dark for 15 min. The proteins were then isolated through a chloroform–methanol protein extraction protocol outlined previously [18] and reconstituted in 4% sodium deoxycholate solution. The protein concentration was quantified using a NanoDrop instrument (Thermo Scientific). The proteins were then digested using two consecutive aliquots of sequencing grade trypsin for three hours and then overnight at 37 °C at the ratio of 1:75 (trypsin to sample protein). Once digestion was complete, SDC was removed through precipitation with 1% formic acid and washed with ethyl acetate. The resulting peptides were lyophilized via SpeedVac (Thermo Scientific), desalted on Pierce peptide desalting spin columns (Thermo Scientific), and resuspended in 0.1% formic acid. A portion of the tryptic peptides (15 µg) was allocated for previously published proteomics measurement [11], while the remaining peptides were lyophilized and then resuspended in the manufacturer-recommended buffer for phosphopeptide enrichment. Phosphopeptide enrichment was carried out using phosphopeptide enrichment kits (Catalog number: A32992). Finally, the enriched phosphopeptides were lyophilized and then resuspended in 0.1% formic acid for phosphoproteomics measurement.

2.2. LC-MS/MS Analysis and Proteome Database Search

All samples were analyzed using an RSLCnano UHPLC system (Thermo Scientific) coupled with a Q Exactive Plus mass spectrometer (Thermo Scientific). The peptides were separated using a biphasic column (strong cation exchange and reversed phase) connected to nanospray emitter with a 75 µm inner diameter that was filled with 25 cm of 1.7 µm Kinetex C18 resin. For the phosphoproteome measurement, a single 1 µg injection of phospho-enriched peptides was analyzed with a 180 min gradient at a salt cut of 500 mM ammonium acetate. The Thermo Xcalibur software was used to acquire MS data

in data-dependent acquisition (DDA) mode with MS2 acquisition set at top 10. All mass spectrometer data were processed in Proteome Discoverer 2.4 using MS Amanda [19] and Percolator [20]. MS data were searched against the *P. virgatum* and *L. bicolor* reference proteome database from DOE Joint Genome Institute (JGI), supplemented with transgenic and common laboratory contaminants sequences. The MS Amanda parameters for phosphopeptide identification were set as follows: MS1 tolerance = 10 ppm; MS2 tolerance = 0.02 Da; missed cleavages = 2; static modification = carbamidomethyl (C, +57.021 Da); dynamic modifications = oxidation (M, +15.995 Da) and phosphorylation (STY) (+79.966 Da). At both the peptide and PSM levels, the false discovery rate (FDR) was set to 1%.

2.3. Data Analysis

To perform differential abundance analysis on phosphorylated peptides, the peptide table was exported from Proteome Discoverer. Then, peptides with phosphorylation modification were extracted from the peptide table. These data were Log₂ transformed, and LOESS normalized using InfernoRDN tool previously published [21]. Additionally, the data matrix was mean centered across all conditions. Only peptides present in at least two out of three replicates (in any experimental conditions) were deemed valid for further analysis. Missing data were imputed using Perseus software [22], with random numbers drawn from a normal distribution with parameters: width = 0.3 and downshift = 2.8. The resulting matrix was subjected to Welch's *t*-test followed by Benjamini–Hochberg FDR correction to evaluate differential abundant proteins between the experimental groups. Finally, the differentially abundant phosphopeptides were mapped to their respective proteins to identify differentially abundant phosphoproteins.

2.4. Bimolecular Fluorescence Complementation (BiFC) Assay

BiFC assay was performed in *Populus* protoplasts as described by Zhang et al., 2020 [23]. In brief, the CDSs of PtLecRLK1 and its substrate candidate proteins were cloned into CFP^c (pUC119-CD3-1068) and VENUSⁿ (pUC119-CD3-1076) vectors through Gateway cloning, respectively. A total of 10 µg of CFP^c-PtLecRLK1 plasmids and 10 µg of VENUSⁿ-substrate plasmids were co-transfected in *Populus* protoplasts. After 18–20 h dark incubation, the reconstructed YFP signals were detected by a Zeiss LSM 710 (Jena, Germany) confocal microscope. ZEN software 2012 SP5 (Jena, Germany) was used for image processing.

3. Results and Discussion

Transgenic expression of *PtLecRLK1* can convert non-host plant species to a host of *L. bicolor*. These transgenic plants can develop a hyphal network between plant cells, improve a plant's fitness in marginal growth conditions, and downregulate pathogenic defense [11]. These findings imply the potential of engineering the mycorrhizal symbiosis for improving plant health or productivity using *PtLecRLK1*. To uncover how *PtLecRLK1* regulates beneficial plant–fungal interaction, we performed phosphoproteomics analysis in transgenic (host) and wild-type (non-host) switchgrass. Because this plasma-membrane receptor is predicted to recognize fungal-cell-wall-derived ligands to suppress plant immunity for long-term colonization, we posit that the resulting signaling cascades are not transient but persistent. Therefore, we sought to characterize the resulting changes in phosphorylation signaling associated with established mycorrhization 2 months post-inoculation.

Across the experimental conditions, 284,588 peptide spectrum matches (PSMs) were identified, out of which 75% had phosphorylation evidence (Figure 1A). These PSMs were mapped to 5140 phosphopeptides in 4469 unique modification sites across 2760 phosphoproteins (Supplemental Table S1). A majority (87%) of these sites belong to amino acid serine, 12% belong to threonine, and the remaining portion belongs to tyrosine (Figure 1A). Most modification sites had a localization probability score of >90% (Figure 1A). A Welch's *t*-test with an FDR correction at $q < 0.05$ and absolute log₂ fold change greater than 1 was implemented to identify phosphopeptide abundances that differed between transgenic *PtLecRLK1* roots and wild-type (WT) roots during *L. bicolor* interaction. This quantitative

analysis identified 1257 differentially abundant phosphopeptides (Figure 1B), of which 610 and 650 phosphopeptides were significantly up- and down-regulated in transgenic *PtLecRLK1* roots compared to wild-type (WT) (Figure 1B) (Supplemental Tables S2 and S3). These phosphopeptides correspond to 603 and 647 differentially abundant phosphoproteins, respectively. The interpretation of quantitative phosphoproteomics can be challenging because differential phosphorylation events could be confused by simultaneous changes in protein abundance. Therefore, proteins previously determined to be differentially regulated in this pairwise comparison [11] were compared against the proteins with a significant change in phosphorylation. This comparison identified 73 phosphorylated proteins that were also observed to have regulated protein abundances, suggesting that the majority of these differentially phosphorylated proteins are regulated exclusively at the post-translational level (Figure 1C). These 73 proteins impacted by several levels of regulation were excluded from the additional analyses. The KEGG enrichment analysis identified MAPK signaling, endocytosis, and phosphatidylinositol signaling as enriched pathways at FDR 0.05 among the proteins that were uniquely regulated at the post-translational level.

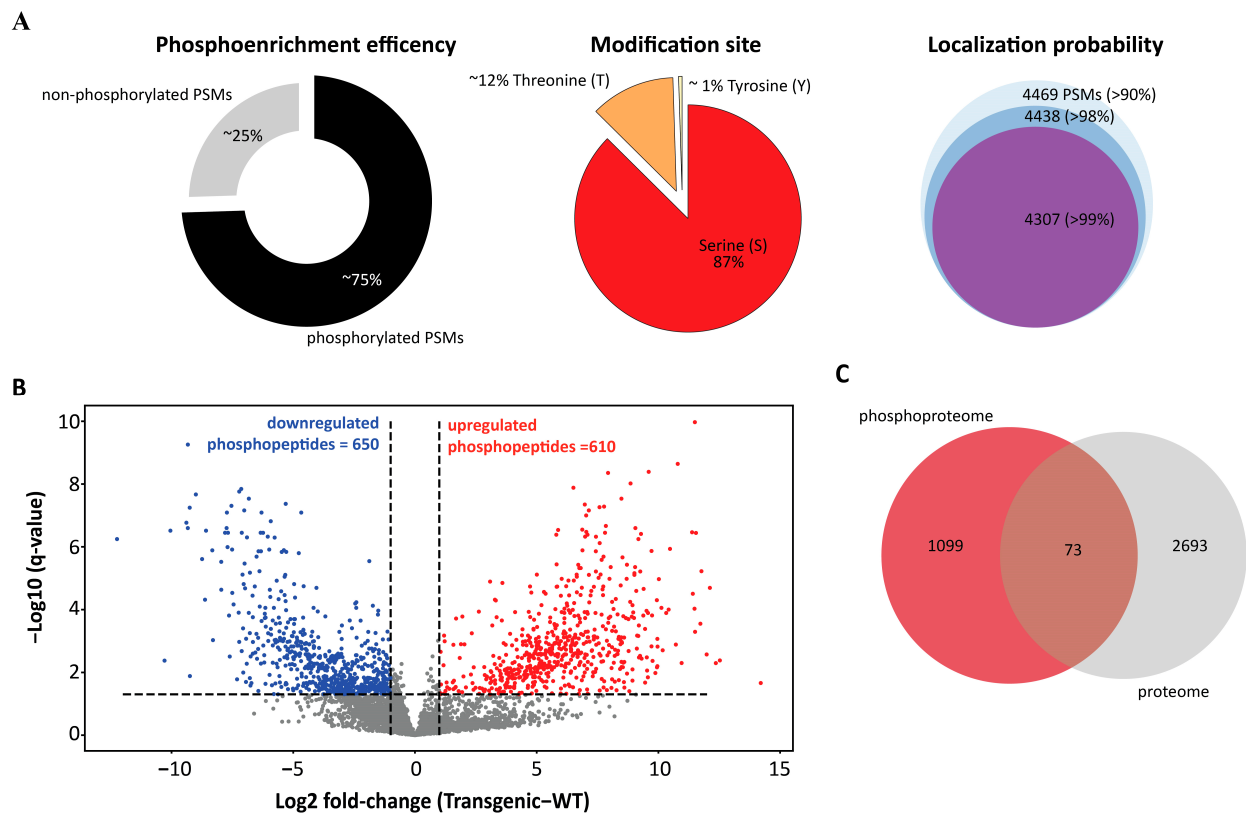


Figure 1. Qualitative and quantitative assessment of phosphoproteomics result from the root samples inoculated with *L. bicolor*. **(A)** Phosphopeptide enrichment efficiency, distribution of phosphosite, and localization probability of phosphorylation modification detected in our study. Most PSMs identified were phosphorylated. Most modified amino acid was serine and majority of the modified site has localization probability greater than 99%. **(B)** Volcano plot showing the differentially abundant phosphopeptides in our comparative phosphoproteomics analysis. Red nodes represent the phosphopeptides that were significantly increased in abundance in *L. bicolor*-inoculated transgenic line compared to WT and blue nodes that represent the phosphopeptides that were significantly decreased in abundance in *L. bicolor*-inoculated transgenic line compared to WT. Significantly changing phosphopeptides are those that pass q-value threshold of 0.05 and log₂ fold change greater than absolute 1. **(C)** Venn diagram comparing the significantly changed phosphopeptides mapped proteins from phosphoproteome analysis to significantly changing proteins from proteome analysis.

In general, a large number of the phosphorylation modifications occurred on proteins and residues that have been previously implicated in plant defense and symbiosis (Supplementary Table S1). For instance, we observed a change in phosphorylation for CERK1, which is one of the most studied RLKs in fungal recognition [14,24,25] because it recognizes chitin found in most fungal cell walls [14,24,25]. In Arabidopsis, *AtCERK1* has been mostly studied for its role in defense-related chitin recognition [24] where chitin recognition results in *AtCERK1* phosphorylation at amino acids S266, S268, S270, S274, and T519 [24]. In our study, LC-MS/MS measurements identified a phosphorylation in the *AtCERK1* homolog (Pavir.6NG335100) and this modification was only observed in transgenic roots colonized by *L. bicolor* (Figure 2A). Sequence alignment analysis shows that the identified S19/T20 phosphorylation aligns well with site S274 from *AtCERK1* (Figure 2B). Chitin-triggered plant defense mediated by CERK1 leads to a MAPK signaling cascade and our analysis identified several phosphorylated proteins involved in the MAPK signaling cascade, which were only observed in transgenic *PtLecRLK1* roots during *L. bicolor* interaction (Figure 2A). In general, this observation suggests that chitin-triggered plant immunity through CERK1 is active. It is plausible that these molecular signatures are a result of having a higher amount of chitin exposed to plant root cells due to enhanced root colonization by transgenic *PtLecRLK1*. Alternatively, it is possible that CERK1 is playing an active role in mediating *L. bicolor* symbiosis within transgenic *PtLecRLK1* roots. Recently, *OsCERK1* was implicated in a symbiotic relationship [15,26] and was shown to be necessary for promoting the colonization of AM fungi during symbiosis [15,26]. Unlike Arabidopsis, rice and switchgrass CERK1 homologs lack LysM domains necessary for chitin recognition. Therefore, it is plausible that the observed phosphorylation alters a coreceptor specific to enabling symbiosis [15,26]. Because we have previously shown that transgenic *PtLecRLK1* Arabidopsis roots can be colonized by *L. bicolor*, the presence or absence of the CERK1 LysM is less likely to be a crucial aspect of this engineered symbiosis and further work is needed to determine the impact of the observed protein modification.

The substrate(s) of *PtLecRLK1* are currently unknown. To identify putative downstream targets, protein–protein interaction (PPI) information was collected for *PtLecRLK1* (Potri.T022200; v3.1) from the STRING database [27,28]. A cGMP-dependent protein kinase (PKG) (Potri.018G084900) was the only PPI reported (Figure 3A). The homolog of this protein in switchgrass (Pavir.1NG172300) was uniquely phosphorylated in transgenic *PtLecRLK1* roots during *L. bicolor* colonization. To further assess whether this PKG is a substrate protein of *PtLecRLK1*, a bimolecular fluorescence complementation (BiFC) assay was performed in poplar protoplasts and the assay suggests *PtLecRLK1* and this PKG interact with each other (Figure 3B). In plants, the role of PKG remains poorly understood. Unlike PKGs expressed in animals, those encoded in plant genomes are structurally unique because they contain an additional type 2C protein phosphatase (PP2C) domain [29]. PP2C-containing proteins are frequently shown to play crucial roles in biotic and abiotic stress responses, plant immunity, and plant development [30]. Recently, the Arabidopsis homolog of this PKG protein was described as an interacting protein of the calcium-associated protein kinase 1 (CAP1) and associated to root ammonium-regulated root hair growth [31]. Interestingly, four ammonium transporters (i.e., two isoforms of AMT1-1 Pavir.1KG399605; Pavir.7KG243500 and two isoforms of AMT 2 Pavir.9KG091401; Pavir.9NG008902) were significantly decreased in phosphorylation abundance in transgenic *PtLecRLK1* switchgrass roots when compared to WT. These AMT proteins are dynamically regulated, existing in either an active or inactive transporter state, and their activity is controlled by the phosphorylation of a conserved threonine residue in the C-terminus [32] (Figure 2B). Phosphorylation of threonine negatively correlates with root ammonium uptake [32]. The decreased phosphorylated protein abundance of all AMT suggests that transgenic *PtLecRLK1* roots during *L. bicolor* colonization is increasing the uptake of ammonium. Inside the plant root cell, ammonium is assimilated into glutamine with the help of glutamine synthetase (GS; Pavir.9KG542200) (Figure 2B), and glutamine acts as a key nitrogen (N) donor for cellular N metabolism and storage. Phosphorylation of GS has been shown

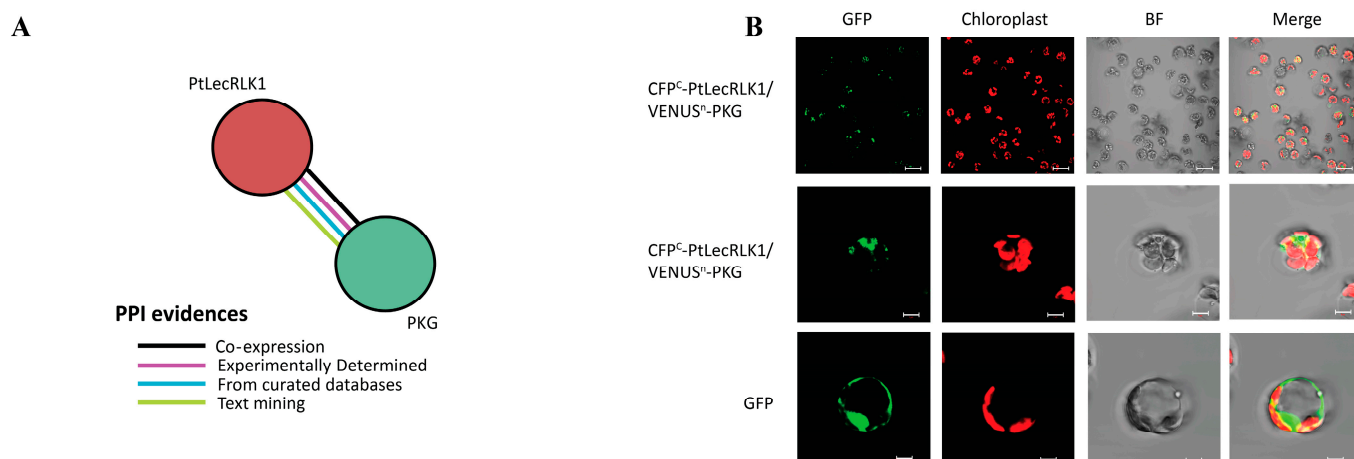


Figure 3. Identification and experimental validation of PtLecRLK1's interacting partner. **(A)** Protein-protein interaction (PPI) obtained for PtLecRLK1 (Potri.T022200; v3.1) from the STRING database. Different lines of evidence for PPI are represented by different color edges. **(B)** Bimolecular fluorescence complementation (BiFC) assay performed in poplar protoplasts showed PtLecRLK1 and cGMP-PK (PKG) interact with each other as they produce green fluorescence. The scale bars for the top panel represent 40 μm , and the scale bars for the middle and bottom panels represents 5 μm .

To further advance our phosphorylation network, PPI information was then collected from the STRING database for PKG. In contrast to our PtLecRLK1 search, there are a much larger number of probable substrates (71 interacting partners identified in poplar with STRING experimentally and co-expression determined score of >0.90), and this suggests that PKG may be a hub kinase for downstream signaling (Supplementary Table S4). Interestingly, among those predicted substrates is a recently discovered susceptibility gene expressed in wheat that has been exploited by a fungal pathogen resulting in stripe rust infection [10]. It has been shown that fungal invasion results in the phosphorylation of TaPsIPK1 protein, which then enters the nucleus and phosphorylates CBF1d to increase fungal susceptibility [10]. Remarkably, inactivating this susceptibility factor has been shown to confer robust rust resistance in a field trial without a negative impact on growth and yield [10]. The switchgrass homologs of TaPsIPK1 (Pavir.1KG067500) and TaCBF1 (Pavir.2NG380900) were found to be uniquely phosphorylated in *L. bicolor*-inoculated transgenic switchgrass (Figure 2A,B).

In addition to these notable changes in phosphorylation status, our global analysis identified many other differentially abundant phosphoproteins related to plant defense, phytohormone signaling such as brassinosteroid signaling and ethylene response, ROS balance, endocytosis, cytoskeleton movement, and proteasomal degradation (Figure 2). Although it is outside the scope of this brief research communication to elaborately describe the implications of these findings for plant–fungal symbiosis, future studies can be targeted to interrogate the functional relevance of these pathways in depth for plant–fungal symbiosis.

4. Conclusions

PTMs, such as phosphorylation, represent a unique layer of regulation utilized by plants to adjust the molecular pathways necessary to either permit or prevent the establishment of a particular microorganism. Overall, this phosphoproteomics study facilitated the identification of phosphorylation-based relevant signaling pathways associated with PtLecRLK1 recognition of *L. bicolor*. This rich dataset along with our previously published multi-omics data have helped to provide a more detailed understanding of how PtLecRLK1 reprograms molecular pathways to facilitate the establishment and maintenance of *L. bicolor* colonization. Moreover, we detected an interaction and a putative PtLecRLK substrate that represents an exciting candidate for further interrogation of this signaling cascade. More broadly, this dataset can be used as a valuable resource for future research that focuses on

cross-species comparisons to see if the *PtLecRLK1*-adjusted molecular pathways are conserved across multiple plant species. In practice, a deeper understanding of plant–fungal signaling pathways will be necessary to selectively engineer beneficial symbiosis while, figuratively speaking, leaving the door closed for pathogens.

Supplementary Materials: The following supporting information can be downloaded at: <https://www.mdpi.com/article/10.3390/cells12071082/s1>, Table S1: Verbose result of identified peptides and proteins at a 1% false discovery rate. Raw abundance values are provided for each peptide; Table S2: Significantly regulated (FDR < 0.05; log₂ FC > 1) phosphopeptides and associated master protein accessions; Table S3: Functional annotation information for regulated phosphoproteins; Table S4: Interacting partners of cGMP-dependent protein kinase (PKG) identified in poplar with STRING experimentally and co-expression determined score of >0.90.

Author Contributions: H.S. conducted the phosphoproteomics sample preparation, mass spectrometry measurement, data analysis, and figures generation, and wrote the manuscript. T.Y., Z.Q., W.M. and J.-G.C. helped with transgenic plant generation and plant growth. W.M. and R.L.H. contributed to the experimental design and provided valuable feedback on the manuscript. J.-G.C. and P.E.A. designed the experiment, assisted in data measurements and analysis, and contributed significantly to manuscript editing. All authors have read and agreed to the published version of the manuscript.

Funding: The design: collection of data, analysis, interpretation, and writing of this manuscript was sponsored by the Genomic Science Program, U.S. Department of Energy, Office of Science, Biological and Environmental Research, as part of the Plant-Microbe Interfaces Scientific Focus Area (<http://pmi.ornl.gov>; accessed on 22 February 2023). Oak Ridge National Laboratory is managed by UT-Battelle, LLC, for the U.S. Department of Energy under contract DE-AC05-00OR22725.

Institutional Review Board Statement: Not applicable.

Informed Consent Statement: Not applicable.

Data Availability Statement: The mass spectrometry data from this study have been deposited at the ProteomeXchange Consortium through the MASSIVE repository at <https://massive.ucsd.edu/>; accessed on 22 February 2023. and can be located under the index MSV000091161.

Acknowledgments: This manuscript has been authored by UT-Battelle, LLC under Contract No. DE-AC05-00OR22725 with the U.S. Department of Energy. The United States Government retains and the publisher, by accepting the article for publication, acknowledges that the United States Government retains a non-exclusive, paid-up, irrevocable, worldwide license to publish or reproduce the published form of this manuscript, or allow others to do so, for United States Government purposes. The Department of Energy will provide public access to these results of federally sponsored research in accordance with the DOE Public Access Plan (<http://energy.gov/downloads/doe-public-access-plan>; accessed on 22 February 2023).

Conflicts of Interest: The authors confirm that there were no competing interests, including financial or commercial relationships, that could potentially influence the results or interpretation of the study.

References

1. Bulgarelli, D.; Rott, M.; Schlaeppli, K.; ver Loren van Themaat, E.; Ahmadinejad, N.; Assenza, F.; Rauf, P.; Huettel, B.; Reinhardt, R.; Schmelzer, E.; et al. Revealing structure and assembly cues for Arabidopsis root-inhabiting bacterial microbiota. *Nature* **2012**, *488*, 91–95. [[CrossRef](#)] [[PubMed](#)]
2. Tringe, S.G.; von Mering, C.; Kobayashi, A.; Salamov, A.A.; Chen, K.; Chang, H.W.; Podar, M.; Short, J.M.; Mathur, E.J.; Detter, J.C.; et al. Comparative Metagenomics of Microbial Communities. *Science* **2005**, *308*, 554–557. [[CrossRef](#)] [[PubMed](#)]
3. Lundberg, D.S.; Lebeis, S.L.; Paredes, S.H.; Yourstone, S.; Gehring, J.; Malfatti, S.; Tremblay, J.; Engelbrekton, A.; Kunin, V.; Del Rio, T.G.; et al. Defining the core Arabidopsis thaliana root microbiome. *Nature* **2012**, *488*, 86–90. [[CrossRef](#)]
4. Edwards, J.; Johnson, C.; Santos-Medellin, C.; Lurie, E.; Podishetty, N.K.; Bhatnagar, S.; Eisen, J.A.; Sundaresan, V. Structure, variation, and assembly of the root-associated microbiomes of rice. *Proc. Natl. Acad. Sci. USA* **2015**, *112*, E911–E920. [[CrossRef](#)]
5. Antolín-Llovera, M.; Petutsching, E.K.; Ried, M.K.; Lipka, V.; Nürnberger, T.; Robatzek, S.; Parniske, M. Knowing your friends and foes—Plant receptor-like kinases as initiators of symbiosis or defence. *New Phytol.* **2014**, *204*, 791–802. [[CrossRef](#)] [[PubMed](#)]
6. Medzhitov, R.; Janeway, C.A., Jr. Decoding the Patterns of Self and Nonsself by the Innate Immune System. *Science* **2002**, *296*, 298–300. [[CrossRef](#)] [[PubMed](#)]

7. Moreira, Z.P.M.; Chen, M.Y.; Ortuno, D.L.Y.; Haney, C.H. Engineering plant microbiomes by integrating eco-evolutionary principles into current strategies. *Curr. Opin. Plant Biol.* **2023**, *71*, 102316. [[CrossRef](#)]
8. Jack, C.N.; Petipas, R.H.; Cheeke, T.E.; Rowland, J.L.; Friesen, M.L. Microbial Inoculants: Silver Bullet or Microbial Jurassic Park? *Trends Microbiol.* **2021**, *29*, 299–308. [[CrossRef](#)]
9. Moore, J.A.M.; Abraham, P.E.; Michener, J.K.; Muchero, W.; Cregger, M.A. Ecosystem consequences of introducing plant growth promoting rhizobacteria to managed systems and potential legacy effects. *New Phytol.* **2022**, *234*, 1914–1918. [[CrossRef](#)]
10. Wang, N.; Tang, C.; Fan, X.; He, M.; Gan, P.; Zhang, S.; Hu, Z.; Wang, X.; Yan, T.; Shu, W.; et al. Inactivation of a wheat protein kinase gene confers broad-spectrum resistance to rust fungi. *Cell* **2022**, *185*, 2961–2974.e19. [[CrossRef](#)]
11. Qiao, Z.; Yates, T.B.; Shrestha, H.K.; Engle, N.L.; Flanagan, A.; Morrell-Falvey, J.L.; Sun, Y.; Tschaplinski, T.J.; Abraham, P.E.; Labbé, J.; et al. Towards engineering ectomycorrhization into switchgrass bioenergy crops via a lectin receptor-like kinase. *Plant Biotechnol. J.* **2021**, *19*, 2454–2468. [[CrossRef](#)] [[PubMed](#)]
12. Labbé, J.; Muchero, W.; Czarniecki, O.; Wang, J.; Wang, X.; Bryan, A.C.; Zheng, K.; Yang, Y.; Xie, M.; Zhang, J.; et al. Mediation of plant–mycorrhizal interaction by a lectin receptor-like kinase. *Nat. Plants* **2019**, *5*, 676–680. [[CrossRef](#)] [[PubMed](#)]
13. Zipfel, C.; Oldroyd, G.E.D. Plant signalling in symbiosis and immunity. *Nature* **2017**, *543*, 328–336. [[CrossRef](#)] [[PubMed](#)]
14. Miya, A.; Albert, P.; Shinya, T.; Desaki, Y.; Ichimura, K.; Shirasu, K.; Narusaka, Y.; Kawakami, N.; Kaku, H.; Shibuya, N. CERK1, a LysM receptor kinase, is essential for chitin elicitor signaling in *Arabidopsis*. *Proc. Natl. Acad. Sci. USA* **2007**, *104*, 19613–19618. [[CrossRef](#)]
15. Carotenuto, G.; Chabaud, M.; Miyata, K.; Capozzi, M.; Takeda, N.; Kaku, H.; Shibuya, N.; Nakagawa, T.; Barker, D.G.; Genre, A. The rice LysM receptor-like kinase OsCERK1 is required for the perception of short-chain chitin oligomers in arbuscular mycorrhizal signaling. *New Phytol.* **2017**, *214*, 1440–1446. [[CrossRef](#)]
16. Deb, S.; Sankaranarayanan, S.; Wewala, G.; Widdup, E.; Samuel, M.A. The S-Domain Receptor Kinase *Arabidopsis* Receptor Kinase2 and the U Box/Armadillo Repeat-Containing E3 Ubiquitin Ligase9 Module Mediates Lateral Root Development under Phosphate Starvation in *Arabidopsis*. *Plant Physiol.* **2014**, *165*, 1647–1656. [[CrossRef](#)]
17. Trontin, C.; Kiani, S.; Corwin, J.A.; Hématy, K.; Yansouni, J.; Kliebenstein, D.J.; Loudet, O. A pair of receptor-like kinases is responsible for natural variation in shoot growth response to mannitol treatment in *Arabidopsis thaliana*. *Plant J.* **2014**, *78*, 121–133. [[CrossRef](#)]
18. Jiang, L.; He, L.; Fountoulakis, M. Comparison of protein precipitation methods for sample preparation prior to proteomic analysis. *J. Chromatogr. A* **2004**, *1023*, 317–320. [[CrossRef](#)]
19. Dorfer, V.; Pichler, P.; Stranzl, T.; Stadlmann, J.; Taus, T.; Winkler, S.; Mechtler, K. MS Amanda, a Universal Identification Algorithm Optimized for High Accuracy Tandem Mass Spectra. *J. Proteome Res.* **2014**, *13*, 3679–3684. [[CrossRef](#)]
20. Käll, L.; Canterbury, J.D.; Weston, J.; Noble, W.S.; MacCoss, M.J. Semi-supervised learning for peptide identification from shotgun proteomics datasets. *Nat. Methods* **2007**, *4*, 923–925. [[CrossRef](#)]
21. Polpitiya, A.D.; Qian, W.J.; Jaitly, N.; Petyuk, V.A.; Adkins, J.N.; Camp, D.G., 2nd; Anderson, G.A.; Smith, R.D. DAnTE: A statistical tool for quantitative analysis of -omics data. *Bioinformatics* **2008**, *24*, 1556–1558. [[CrossRef](#)] [[PubMed](#)]
22. Tyanova, S.; Temu, T.; Sinitcyn, P.; Carlson, A.; Hein, M.Y.; Geiger, T.; Mann, M.; Cox, J. The Perseus computational platform for comprehensive analysis of (prote)omics data. *Nat. Methods* **2016**, *13*, 731–740. [[CrossRef](#)]
23. Zhang, J.; Xie, M.; Li, M.; Ding, J.; Pu, Y.; Bryan, A.C.; Rottmann, W.; Winkler, K.A.; Collins, C.M.; Singan, V.; et al. Overexpression of a Prefoldin beta subunit gene reduces biomass recalcitrance in the bioenergy crop *Populus*. *Plant Biotechnol. J.* **2020**, *18*, 859–871. [[CrossRef](#)]
24. Petutschnig, E.K.; Jones, A.M.; Serazetdinova, L.; Lipka, U.; Lipka, V. The lysin motif receptor-like kinase (LysM-RLK) CERK1 is a major chitin-binding protein in *Arabidopsis thaliana* and subject to chitin-induced phosphorylation. *J. Biol. Chem.* **2010**, *285*, 28902–28911. [[CrossRef](#)] [[PubMed](#)]
25. Cao, Y.; Liang, Y.; Tanaka, K.; Nguyen, C.T.; Jedrzejczak, R.P.; Joachimiak, A.; Stacey, G. The kinase LYK5 is a major chitin receptor in *Arabidopsis* and forms a chitin-induced complex with related kinase CERK1. *eLife* **2014**, *3*, e03766. [[CrossRef](#)] [[PubMed](#)]
26. Zhang, X.; Dong, W.; Sun, J.; Feng, F.; Deng, Y.; He, Z.; Oldroyd, G.E.; Wang, E. The receptor kinase CERK1 has dual functions in symbiosis and immunity signalling. *Plant J.* **2014**, *81*, 258–267. [[CrossRef](#)]
27. von Mering, C.; Huynen, M.; Jaeggi, D.; Schmidt, S.; Bork, P.; Snel, B. STRING: A database of predicted functional associations between proteins. *Nucleic Acids Res.* **2003**, *31*, 258–261. [[CrossRef](#)]
28. Szklarczyk, D.; Gable, A.L.; Nastou, K.C.; Lyon, D.; Kirsch, R.; Pyysalo, S.; Doncheva, N.T.; Legeay, M.; Fang, T.; Bork, P.; et al. The STRING database in 2021: Customizable protein-protein networks, and functional characterization of user-uploaded gene/measurement sets. *Nucleic Acids Res.* **2021**, *49*, D605–D612. [[CrossRef](#)]
29. Shen, Q.; Zhan, X.; Yang, P.; Li, J.; Chen, J.; Tang, B.; Wang, X.; Hong, Y. Dual Activities of Plant cGMP-Dependent Protein Kinase and Its Roles in Gibberellin Signaling and Salt Stress. *Plant Cell* **2019**, *31*, 3073–3091. [[CrossRef](#)]
30. Yang, Q.; Liu, K.; Niu, X.; Wang, Q.; Wan, Y.; Yang, F.; Li, G.; Wang, Y.; Wang, R. Genome-wide Identification of PP2C Genes and Their Expression Profiling in Response to Drought and Cold Stresses in *Medicago truncatula*. *Sci. Rep.* **2018**, *8*, 12841. [[CrossRef](#)]
31. Yu, J.; Ma, X.; Wang, L.; Dong, N.; Wang, K.; You, Q.; Xu, Y.; Wang, C.; Dong, Z.; Shi, Z.; et al. *Arabidopsis* CAP1 mediates ammonium-regulated root hair growth by influencing vesicle trafficking and the cytoskeletal arrangement in root hair cells. *J. Genet. Genom.* **2022**, *49*, 986–989. [[CrossRef](#)] [[PubMed](#)]

32. Lanquar, V.; Frommer, W.B. Adjusting ammonium uptake via phosphorylation. *Plant Signal. Behav.* **2010**, *5*, 736–738. [[CrossRef](#)] [[PubMed](#)]
33. Huyghe, D.; Denninger, A.R.; Voss, C.M.; Frank, P.; Gao, N.; Brandon, N.; Waagepetersen, H.; Ferguson, A.D.; Pangalos, M.; Doig, P.; et al. Phosphorylation of Glutamine Synthetase on Threonine 301 Contributes to Its Inactivation During Epilepsy. *Front. Mol. Neurosci.* **2019**, *12*, 120. [[CrossRef](#)] [[PubMed](#)]

Disclaimer/Publisher’s Note: The statements, opinions and data contained in all publications are solely those of the individual author(s) and contributor(s) and not of MDPI and/or the editor(s). MDPI and/or the editor(s) disclaim responsibility for any injury to people or property resulting from any ideas, methods, instructions or products referred to in the content.